



# Infrared light induced photoelectrocatalytic application via graphene oxide coated thermoelectric device



Songmei Sun, Wenzhong Wang\*, Dong Jiang, Ling Zhang, Jing Zhou

State Key Laboratory of High Performance Ceramics and Superfine Microstructure, Shanghai Institute of Ceramics, Chinese Academy of Sciences, 1295 Dingxi Road, Shanghai 200050, PR China

## ARTICLE INFO

### Article history:

Received 22 January 2014

Received in revised form 20 March 2014

Accepted 6 April 2014

Available online 14 April 2014

### Keywords:

Graphene oxide

Bismuth tungstate

Photoelectrocatalytic

Infrared light

## ABSTRACT

The infrared light, accounting for almost half of the sun light, has not been utilized effectively by traditional semiconductor-based solar energy conversion technology that is mainly active in the region from ultraviolet to visible light. Thermoelectric device coupled with infrared-active photothermal material provides a unique way to convert the infrared light into electricity. Here we designed a new strategy by coating graphene oxide on a thermoelectric device to realize infrared light generated electricity. By this approach, we successfully achieved harvesting infrared-generated photo-voltage to improve the efficiency of solar light driven photocatalysis via a photoelectrocatalytic process.

© 2014 Elsevier B.V. All rights reserved.

## 1. Introduction

Solar energy conversion is one of the most promising ways to solve the current energy crisis. It has been widely reported that solar radiation can be converted into electricity or chemical fuels by semiconductor photovoltaic or photocatalytic materials [1–6]. However, most of these solar energy conversion materials, such as Si, TiO<sub>2</sub>, II–VI, III–V, IV–VI and I–III–VI based semiconductors etc. [7–12], are only active in the region from ultraviolet to near infrared light. The infrared light, accounting for almost half of the sun light, has not been utilized effectively by the current semiconductor-based solar technology. To improve the solar energy utilization efficiency, other technologies should be developed.

The infrared light typically dissipates their energy as heat by photothermal effect. The most obvious way to harness the infrared solar energy is converting this heat into other useful power source, such as electricity. Thermoelectric (TE) device makes this conversion possible [13]. However, the surface of commercial TE device is insufficient for the infrared light absorption. Expansion of the infrared light absorption of the TE devices is required for improving their efficiency. This demand inspired us to explore the possibility of integrating graphene oxide (GO) on the surface of the TE device to improve the photo-thermo-electric conversion efficiency. As a novel material, GO was recently recognized as possessing

surprisingly strong infrared light absorption [14]. This absorption is a new phenomenon specific to graphene-based structures, which suggests a new means for harvesting solar energy. Based on this performance, GO was found exhibiting excellent infrared photothermal conversion that can directly transform infrared photoenergy into thermal energy, bringing promising signs in solar energy utilization with high-efficiency [15,16]. Furthermore, GO is easy to produce from natural graphite by chemical oxidation procedure through which natural graphite can be effectively oxidized and exfoliated with the introduction of oxygen-containing functional groups [17]. The presence of oxygen-containing functional groups in GO endows it strongly hydrophilic. This is important for obtaining a stable and homogeneous GO dispersion in water that would be subsequently deposited on the surface of TE device by common methods such as drop-casting, spraying, or spin-coating [18].

Herein we demonstrate that the photothermal effect of GO can be utilized as a heat source for TE devices for the first time. The GO coated TE device provides a new approach to convert the infrared light into electricity. By this approach, the infrared-generated photo-voltage could be used for improving the efficiency of solar light driven photocatalysis via a photoelectrocatalytic process.

## 2. Experimental

**Synthesis:** The GO was synthesized according to the modification of Hummers' methods and the process was described previously

\* Corresponding author. Tel.: +86 21 5241 5295; fax: +86 21 5241 3122.  
E-mail address: [wzwang@mail.sic.ac.cn](mailto:wzwang@mail.sic.ac.cn) (W. Wang).

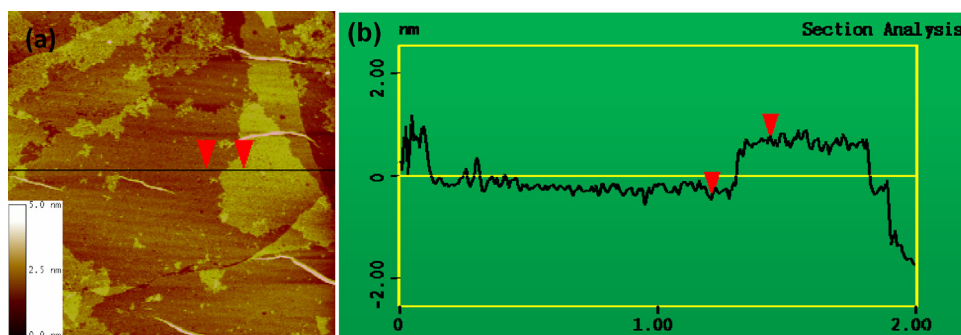


Fig. 1. (a) AFM image of the graphene oxide, (b) the corresponding section analyses of a.

[19,20]. The obtained GO was dispersed in water (0.5 g/L) and subsequently sonicated for 1 h. The GO coated commercial TE device was prepared by drop-coating method using this GO dispersion. The  $\text{Bi}_2\text{WO}_6$  film electrode was synthesized according to the previous report [21]. The commercial TE device is p–n junction type (n:  $\text{Bi}_2\text{Te}_3$ – $\text{Bi}_2\text{Se}_3$  solid–solution; p:  $\text{Bi}_2\text{Te}_3$ – $\text{Sb}_2\text{Te}_3$  solid–solution) with a laminar size of  $3\text{ cm} \times 3\text{ cm}$ .

**Characterization:** Atomic force microscopy (AFM) was acquired by using a NanoScope SPM (Digital instrument Inc.) with Picoscope v5.3.3 software. Samples for AFM images were prepared by depositing GO on a freshly cleaved mica surface and allowing them to dry in air. The infrared thermal image of the TE device was performed by Flir T335 Thermal Imaging Camera. Fourier transform infrared (FTIR) spectroscopy was performed with a spectrophotometer (Nicolet 380, Thermo, USA) with the KBr pellet technique.

**Electrochemical measurements:** *I*–*V* measurements of TE devices were performed on a CHI 660D electrochemical workstation (Shanghai Chenhua, China) by using two electrodes without a reference electrode under the irradiation of 100 W PHILIPS infrared lamp. *I*–*V* measurements of the TE device coupled photocatalytic system were performed on a CHI 660D electrochemical workstation (Shanghai Chenhua, China) using a standard three-electrode cell with a working electrode, a platinum wire as counter electrode, and a standard saturated calomel electrode (SCE) in saturated KCl as reference electrode. The simulated solar light source employed was a 500 W xenon light.

**Photocatalytic test:** Photocatalytic test of the TE device assisted photocatalytic system was evaluated by the degradation of phenol under the irradiation of a 500 W Xe lamp in a quartz reactor. The reactor containing 10 mL of phenol (8 mg/L) solution was placed 10 cm away from a 500 W Xe lamp. The concentration of phenol was monitored by measuring the absorbance at 269 nm using a Hitachi U-3010 UV–visible spectrophotometer.

### 3. Results and discussion

The proof-of-concept experiments were performed by coating GO sheets on a commercial TE device. Fig. 1a is the AFM image of the GO used in this study. The cross section analysis (Fig. 1b) of the AFM image indicates a height of 1 nm for the GO sheets, indicating the GO sheets used in this study are monolayer [22–24]. The monolayer GO sheets are advantageous for obtaining a stable and homogeneous GO dispersion for integrating with the TE device. Furthermore, GO has a large number of oxygen-containing functional groups such as the C–OH group which could largely absorb infrared light [25,26]. Recent studies indicated GO is amphiphilic and surface active. It is apt to adhere to interfaces and lower the interfacial energy [18,27,28]. These features facilitate GO to form a uniform and stable coating on the surface of TE device by a drop-casting method. As anticipated, the prepared GO sheets exhibited excellent infrared light absorption property (Fig.

S1 in the Supporting information). For this reason, the surface temperature of the GO coated TE device increased quickly under the irradiation of infrared light, which is advantageous for the thermoelectric conversion. Fig. 2a is the infrared thermal image of the GO coated TE device under the irradiation of a 100 W infrared lamp (0.78–2.8  $\mu\text{m}$ ). The uneven distribution of the surface temperature is attributed to the different thickness of the coated GO. The area which possesses thicker GO coating attend a temperature of  $96^\circ\text{C}$  within 5 min, meanwhile the temperature of its adjacent area with thinner GO coating is  $86^\circ\text{C}$ . From Fig. 2a, it is obvious the infrared thermal image and the photograph (inset of Fig. 2a) exhibited the same pattern, which comes from the thickness nonuniformity of GO coating on the surface. This indicates coating GO on the surface of the TE device could evidently improve the thermal response of the TE device. For comparison, the infrared thermal image of the bare TE device without GO coating was also detected, as shown in Fig. 2b. It exhibits a much lower temperature of about  $74^\circ\text{C}$  under the same conditions, further proving the enhancement of thermal response of the TE device by integration of GO.

Fig. 3a shows representative current (*I*)–voltage (*V*) characteristics of TE device measured in the dark and under illumination of infrared light. The linear *I*–*V* curve suggests an ohmic contact in the TE device [29]. It was observed that both in darkness and under illumination, the TE device shows almost the same resistance, because the slope of the *I*–*V* curve was only slightly enhanced. It was also found the GO coated TE device exhibits a higher resistance under the potential of 0–0.2 V. The increased resistance is caused by the obvious improved surface temperature of the GO coated TE device under the illumination of infrared light. Because of this improved temperature, a more than twice increase in current is observed (Fig. 3a) for the GO coated TE device, comparing with bare TE device under the same infrared light irradiation. This increased current can be ascribed to the photothermal effect from the integrated GO. In order to further study the effect of GO coating on the thermoelectric response of the TE device, the discussion of current vs. time under the illumination of infrared light is displayed in Fig. 3b. A constant bias potential of 0.002 V is maintained for both of the TE device and the GO coated TE device during the measurement. As shown in Fig. 3b, the thermal induced current is immediately generated as a result of infrared light irradiation. The maximum current is 52 mA for bare TE device, while it is 87 mA for the GO coated TE device after irradiation for 5 min. It is observed the current increase of GO coated TE device is much faster than the bare device in the first 100 s from Fig. 3b. The essential reason for the improvement of the thermal response of GO coated TE device is that the GO coating favors the infrared light absorption to increase the surface temperature of the TE device rapidly.

Though the intensity of electricity from the TE device by infrared light irradiation is diminutive, it is useful to imposing on photovoltaic device to increase the photoconversion efficiency, such as in the photoelectrocatalytic applications. For a widely

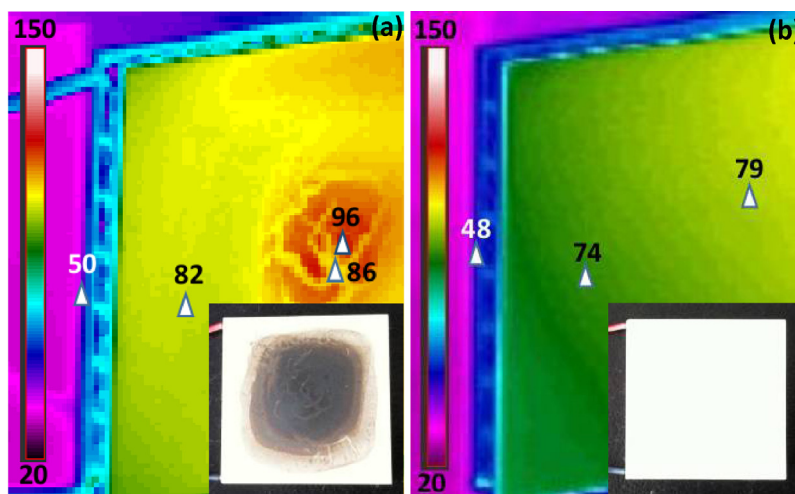


**Fig. 2.** The infrared thermal image of the GO coated TE device (a) and the bare TE device (b) under the irradiation of a 100 W infrared lamp, Inset is the corresponding photograph of the TE device.

studied photocatalyst  $\text{Bi}_2\text{WO}_6$  as an example, it was found the infrared light generated voltage from the TE device could largely improve the simulated solar light induced photocurrent of  $\text{Bi}_2\text{WO}_6$  film and then evidently improve its photocatalytic performance.

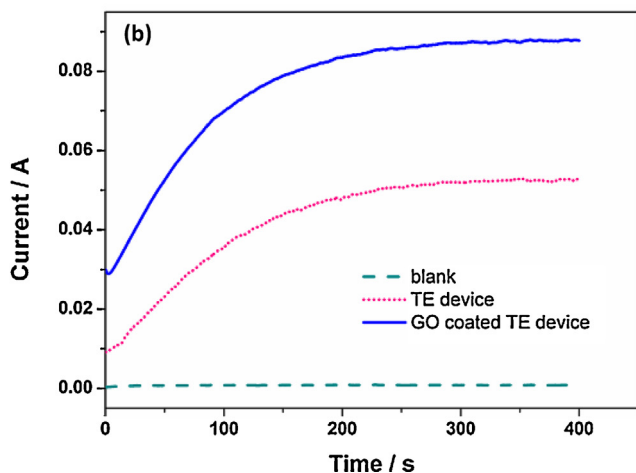
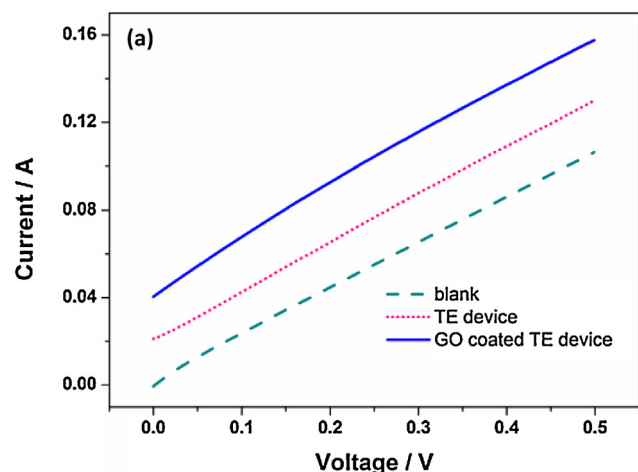


**Fig. 3.** (a) Current–voltage plots and (b) current time dependence of TE device before and after GO coating under irradiation of infrared light.

**Fig. 4** shows the current–voltage ( $I$ – $V$ ) curves for the  $\text{Bi}_2\text{WO}_6$  film in the dark and under simulated solar light illumination. It was observed from **Fig. 4** that the photocurrent from the  $\text{Bi}_2\text{WO}_6$  film was gradually increased along with the increase of imposed potential under the illumination of simulated solar light. This photocurrent comes from the simulated solar light excited electrons of the  $\text{Bi}_2\text{WO}_6$  photocatalysts. When a bias potential from the GO coated TE device under infrared light irradiation was imposed on the  $\text{Bi}_2\text{WO}_6$  film, the current from the  $\text{Bi}_2\text{WO}_6$  film was evidently increased. The current under this situation shows an increase of 5.6 times compared with the state without the assistance of GO coated TE device. The evidently improved current of the  $\text{Bi}_2\text{WO}_6$  film is advantageous for its photocatalytic application.

The photocatalytic performance was evaluated by the degradation of phenol under simulated solar light irradiation. **Fig. S2** displays the temporal evolution of the phenol absorption spectrum before and after the degradation over the GO coated TE device assisted  $\text{Bi}_2\text{WO}_6$  photocatalyst. The rapid decrease of phenol absorption at a wavelength of 269 nm indicates the  $\text{Bi}_2\text{WO}_6$  photocatalyst exhibits excellent photocatalytic degradation of phenol under the assistance of GO coated TE device. **Fig. 5** shows photocatalytic efficiency of phenol decomposition by different

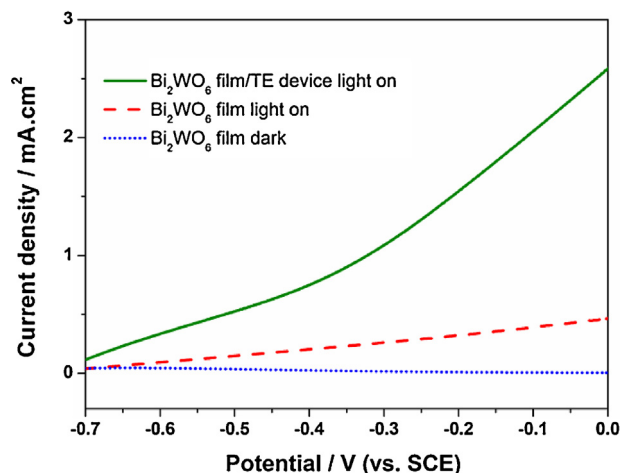


**Fig. 4.** Photocurrent densities of  $\text{Bi}_2\text{WO}_6$  film with and without the assistant of GO coated TE device under simulated solar light in 0.5 M  $\text{Na}_2\text{SO}_4$  solution.

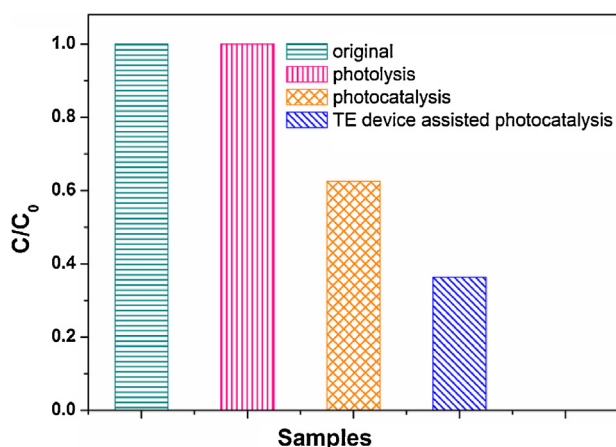


Fig. 5. Phenol degradation efficiencies on  $\text{Bi}_2\text{WO}_6$  in different processes.  $C$  was the absorbance of phenol at the wavelength of 269 nm and  $C_0$  was the absorbance of phenol after the adsorption equilibrium on  $\text{Bi}_2\text{WO}_6$  samples before irradiation.

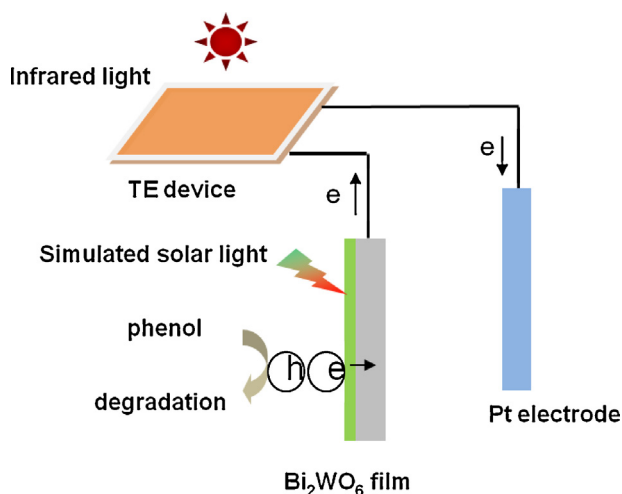


Fig. 6. The schematic illustration of the TE device assisted  $\text{Bi}_2\text{WO}_6$  photocatalytic system.

photocatalytic process on  $\text{Bi}_2\text{WO}_6$  under simulated solar light irradiation for 1 h. It was found the photocatalytic performance under the assistance of GO coated TE device is increased about 1.7 times compared with that without the assistance of TE device. A necessary step for semiconductor photocatalytic process is the generation and separation of electron-hole pairs. The enhanced photocatalytic performance of the GO coated TE device assisted system is attributed to the imposed bias potential from the TE device under infrared light irradiation. The schematic illustration of the TE device assisted photocatalytic system was shown in Fig. 6. Under the electric potential generated from the TE device, the simulated solar light induced electrons from the photocatalyst film could escape to the counter electrode efficiently. This process could largely decrease the recombination rate of the photogenerated electron-hole pairs and increase the photocatalytic performance. This photoelectrocatalytic system is different from the traditional photoelectrocatalytic device, which was realized only by light irradiation without the assistant of external voltage. This coupled photo-thermo-electric conversion system could also be applied to infrared light induced water splitting, which is now understudying in our group.

#### 4. Conclusions

Graphene oxide, which exhibits strong infrared light absorption and excellent photothermal conversion effect, was selected to integrate with commercial TE device to realize infrared light induced electricity. This electricity was harvested to realize photoelectrocatalytic technology without external applied voltage. It was found the infrared light generated photo-voltage from the GO coated TE device could highly improve the simulated solar light driven photocatalysis via a photoelectrocatalytic process. This work provides an innovative and principal method to realize photoelectrocatalytic technology without external applied voltage.

#### Acknowledgment

This work was financially supported by the National Natural Science Foundation of China (Grant Nos. 51102262, 51272269) and the Science Foundation for Youth Scholar of State Key Laboratory of High Performance Ceramics and Superfine Microstructures (Grant No. SKL201204).

#### Appendix A. Supplementary data

Supplementary data associated with this article can be found, in the online version, at <http://dx.doi.org/10.1016/j.apcatb.2014.04.009>.

#### References

- [1] H.E. Katz, A.J. Lovinger, J. Johnson, C. Kloc, T. Siegrist, W. Li, Y.Y. Lin, A. Dodabalapur, *Nature* 404 (2000) 478–481.
- [2] T. Choi, S. Lee, Y.J. Choi, V. Kiryukhin, S.W. Cheong, *Science* 324 (2009) 63–66.
- [3] I. Gonzalez-Valls, M. Lira-Cantu, *Energy Environ. Sci.* 2 (2009) 19–34.
- [4] A.W. Hains, Z. Liang, M.A. Woodhouse, B.A. Gregg, *Chem. Rev.* 110 (2010) 6689–6735.
- [5] S.U.M. Khan, M. Al-Shahry, W.B. Ingler, *Science* 297 (2002) 2243–2245.
- [6] A. Kudo, Y. Miseki, *Chem. Soc. Rev.* 38 (2009) 253–278.
- [7] S.A. McDonald, G. Konstantatos, S. Zhang, P.W. Cyr, E.J.D. Klem, L. Levina, E.H. Sargent, *Nat. Mater.* 4 (2005) 138–142.
- [8] M.G. Panthani, V. Akhavan, B. Goodfellow, J.P. Schmidtke, L. Dunn, A. Dodabalapur, P.F. Barbara, B.A. Korgel, *J. Am. Chem. Soc.* 130 (2008) 16770–16777.
- [9] R.R. King, D.C. Law, K.M. Edmondson, C.M. Fetzer, G.S. Kinsey, H. Yoon, R.A. Sherif, N.H. Karam, *Appl. Phys. Lett.* 90 (2007) 183516–183523.
- [10] M.D. Kelzenberg, S.W. Boettcher, J.A. Petykiewicz, D.B. Turner-Evans, M.C. Putnam, E.L. Warren, J.M. Spurgeon, R.M. Briggs, N.S. Lewis, H.A. Atwater, *Nat. Mater.* 9 (2010) 239–244.
- [11] I. Gur, N.A. Fromer, M.L. Geier, A.P. Alivisatos, *Science* 310 (2005) 462–465.
- [12] K. Zhu, N.R. Neale, A. Miedaner, A.J. Frank, *Nano Lett.* 7 (2007) 69–74.
- [13] A. Majumdar, *Science* 303 (2004) 777–778.
- [14] M. Acik, G. Lee, C. Mattevi, M. Chhowalla, K. Cho, Y.J. Chabal, *Nat. Mater.* 9 (2010) 840–845.
- [15] J.T. Robinson, S.M. Tabakman, Y. Liang, H. Wang, H.S. Casalongue, D. Vinh, H. Dai, *J. Am. Chem. Soc.* 133 (2011) 6825–6831.
- [16] C. Wu, J. Feng, L. Peng, Y. Ni, H. Liang, L. He, Y. Xie, *J. Mater. Chem.* 21 (2011) 18584–18591.
- [17] S. Park, R.S. Ruoff, *Nat. Nanotechnol.* 4 (2009) 217–224.
- [18] F. Kim, L.J. Cote, J.X. Huang, *Adv. Mater.* 22 (2010) 1954–1958.
- [19] W.S. Hummers, R.E. Offeman, *J. Am. Chem. Soc.* 80 (1958) 1339.
- [20] E. Gao, W. Wang, M. Shang, J. Xu, *Phys. Chem. Chem. Phys.* 13 (2011) 2887–2893.
- [21] S. Sun, W. Wang, L. Zhang, *J. Phys. Chem. C* 116 (2012) 19413–19418.
- [22] G. Williams, B. Seger, P.V. Kamat, *ACS Nano* 2 (2008) 1487–1491.
- [23] C. Gómez-Navarro, R.T. Weitz, A.M. Bittner, M. Scolari, A. Mews, M. Burghard, K. Kern, *Nano Lett.* 7 (2007) 3499–3503.
- [24] S. Stankovich, D.A. Dikin, R.D. Piner, K.A. Kohlhaas, A. Kleinhammes, Y. Jia, Y. Wu, S.T. Nguyen, R.S. Ruoff, *Carbon* 45 (2007) 1558–1565.
- [25] D. Chen, H. Feng, J. Li, *Chem. Rev.* 112 (2012) 6027–6053.
- [26] C. Huang, C. Li, G. Shi, *Energy Environ. Sci.* 5 (2012) 8848–8868.
- [27] J. Kim, L.J. Cote, F. Kim, W. Yuan, K.R. Shull, J.X. Huang, *J. Am. Chem. Soc.* 132 (2010) 8180–8186.
- [28] J. Kim, L.J. Cote, J. Huang, *Acc. Chem. Res.* 45 (2012) 1356–1364.
- [29] A. Datta, S.K. Panda, S. Chaudhuri, *J. Phys. Chem. C* 111 (2007) 17260–17264.